

AperTO - Archivio Istituzionale Open Access dell'Università di Torino

Myostatin regulates the fibrogenic phenotype of hepatic stellate cells via c-jun N-terminal kinase activation

This is a pre print version of the following article:

Original Citation:

Availability:

This version is available <http://hdl.handle.net/2318/1717634> since 2019-11-25T17:39:21Z

Published version:

DOI:10.1016/j.dld.2019.03.002

Terms of use:

Open Access

Anyone can freely access the full text of works made available as "Open Access". Works made available under a Creative Commons license can be used according to the terms and conditions of said license. Use of all other works requires consent of the right holder (author or publisher) if not exempted from copyright protection by the applicable law.

(Article begins on next page)

Myostatin regulates the fibrogenic phenotype of hepatic stellate cells via c-jun N-terminal kinase activation

Wanda Delogua,¹, Alessandra Caligiuri ^{a,1}, Angela Provenzano^a, Chiara Rossoc, Elisabetta Bugianesic, Andrea Corattid, Jose Macias-Barragana,², Sara Galastri ^{a,3}, Giovanni Di Mairaa, Fabio Marraa,^{b,*}

^a Dipartimento di Medicina Sperimentale Clinica, University of Florence, Florence, Italy ^b Research Center Denothe, University of Florence, Florence, Italy ^c Dipartimento di Scienze Mediche, University of Turin, Turin, Italy ^d SOD Chirurgia Oncologia a indirizzo robotico, Azienda Ospedaliero-Universitaria Careggi, Florence, Italy

Abstract

Background & aims: Myostatin is mainly expressed in skeletal muscle, where it negatively regulates trophism. This myokine is implicated in the pathophysiology of nonalcoholic steatohepatitis, an emerg-ing cause of liver fibrosis. In this study we explored the effects of myostatin on the biology of hepatic stellate cells.

Methods: The effects of myostatin were assessed both in LX-2 and in human primary stellate cells. Cell migration was determined in Boyden chambers. Activation of intracellular pathways was evaluated by Western blotting. Procollagen type 1 secretion was measured by enzyme immunoassay. The role of c-Jun N-terminal kinase was assessed by pharmacologic and genetic inhibition.

Results: Activin receptor-2B was up-regulated in livers of mice with experimental fibrosis, and detectable in human stellate cells. Serum myostatin levels increased in a model of acute liver injury. Myostatin reduced HSC proliferation, induced cell migration, and increased expression of procollagen type1, tis-sue inhibitor of metalloproteinase-1, and transforming growth factor- ₁. Myostatin activated different signaling pathways, including c-Jun N-terminal kinase and Smad3. Genetic and/or pharmacologic inhi-bition of c-Jun N-terminal kinase activity significantly reduced cell migration and procollagen secretion in response to myostatin.

Conclusions: Activation of activin receptor-2B by myostatin modulates the fibrogenic phenotype of human stellate cells, indicating that a myokine may be implicated in the pathogenesis of hepatic fibrosis.

Introduction

Myostatin, also known as growth differentiation factor-8, is a highly conserved protein belonging to the transforming factor- β family. Expression of myostatin is detected primarily in skeletal muscle, and is a negative modulator of muscle growth and trophism [1]. In fact, mutations or targeted deletion in mammalian species cause muscle hypertrophy and hyperplasia [2]. Accordingly, myostatin has been implicated in the pathogenesis of muscle wasting in different conditions, including cancer cachexia [3]. The action of myostatin is mediated by interaction with activin receptor-2B (ActR2B) [4] and results in activation of a Smad3/4 complex and its translocation to the nucleus, where target genes are activated. Recent findings suggest a possible involvement of myostatin in the abnormalities associated with the metabolic syndrome. Myostatin-deficient mice have a significant reduction in fat accumulation, despite normal food intake, and show improved insulin sensitivity in conditions of obesity [5,6]. In humans, elevated expression levels of myostatin have been reported in the muscle of patients with type 2 diabetes, and myostatin expression is reduced in the skeletal muscle of obese individuals undergoing weight loss [1,7,8]. Skeletal muscle is a relevant part of the network coordinating metabolism and participates in the complex alterations occurring in the metabolic syndrome and insulin resistance [9]. Nonalcoholic fatty liver disease (NAFLD) is the hepatic counterpart of this disorder and is characterized by accumulation of fat, predominantly in the form of triglycerides [10]. NAFLD is associated with a higher risk of liver-related and all-cause mortality, due to the occurrence of nonalcoholic steatohepatitis (NASH), which may lead to the appearance of cirrhosis and its complications, including hepatocellular carcinoma [11]. Recent studies have indicated that the presence of fibrosis is a major risk factor for progression of NAFLD and mortality [12,13]. Thus, understanding the molecular and cellular mechanisms leading to fibrosis in this setting is of crucial importance to design appropriate management strategies for patients with NASH. Compelling evidence in the past two decades has highlighted the pivotal role played by hepatic stellate cells (HSC) as the key effectors in the pathogenesis of fibrosis in different chronic liver diseases, including NASH [14,15]. Although fibrosis is the ultimate outcome of all chronic liver diseases, there is accumulating evidence for disease- and context-specific mechanisms that may modulate or drive hepatic fibrogenesis [16]. In this respect, no information is currently available concerning a possible contribution of myokines, i.e. cytokines predominantly expressed in skeletal muscle, on the cellular and molecular mechanisms of fibrogenesis. Here we show that myostatin is a novel modulator of the biology of HSC, differentially affecting proliferation, migration and expression of extracellular matrix components, via activation of the c-Jun N-terminal kinase (JNK) pathway.

Materials and methods

Materials

Recombinant human myostatin and platelet-derived growth factor-BB were from Peprotech (Rocky Hill, NJ). Monoclonal anti-bodies against vinculin and β -actin were from Sigma Chemical Co. (St. Louis, MO). Polyclonal antibodies against total- and phospho-rylated JNK were from Santa Cruz Biotechnology (Santa Cruz, CA). Phosphorylation-specific antibodies against ERK1/2, Akt (Ser473) and Smad3 were from Cell Signaling Technology (Danvers, MA). SP600125 was from Sigma Chemical Co. (Sigma Aldrich Spa, Milano, Italy). Procollagen type 1 C-peptide (PIP) EIA kit was purchased from Takara Bio (Mountain View, CA). The anti-Activin Receptor Type IIB antibody – N-terminal (ab135635) was purchased from Abcam (Cambridge, UK). Anti- α -smooth muscle actin antibodies were from Sigma.

Cell cultures

LX-2 cells were a kind gift of Dr. Scott L. Friedman (Mount Sinai School of Medicine, New York, NY). Primary human HSC were isolated as previously described in detail and used after complete transition towards a myofibroblast-like phenotype [17]. Both cell types were cultured in Iscove's modified Dulbecco's medium supplemented with 2.0 mmol/L of glutamine, 0.1 mmol/L of nonessential amino acids, 1.0 mmol/L of sodium pyruvate, antibiotic–antimycotic solution and 20% foetal bovine serum (all provided by Gibco Laboratories, Grand Island, NY). Cells were serum deprived for 48 h before all the experiments. MTT assay Cell proliferation was determined measuring the cellular metabolic activity using the 3-(4,5-dimethylthiazolyl-2)-2, 5-diphenyltetrazolium bromide (MTT) assay, as described elsewhere [18]. Serum-starved LX-2 cells were exposed to different concentrations of myostatin or 10 ng/ml PDGF-BB, used as positive control, for 24, 48, or 72 h. Cells were then treated with MTT (5 mg/ml in PBS and then with lysis solution (20% (w/v) SDS, 50% (v/v) N,N-dimethylformamide, 2% (v/v) acetic acid and 25 mM HCl, pH 4.7). Samples were read at 590 nm in a Multiskan FC plate reader.

Migration assay

These experiments were performed essentially as previously described, using Boyden chambers equipped with 8- μ m porosity polyvinylpyrrolidone-free polycarbonate filters [17]. When inhibitors were used, cultured cells were treated with drugs to be tested or with their vehicle for 15 min before trypsinization, and equal concentrations were added to both chambers of the Boyden apparatus.

RNA isolation and quantitative real time PCR

Total RNA was isolated using the Nucleo Spin RNA kit (Macherey-Nagel, Duren, Germany) and reverse-transcribed by MMLV reverse transcriptase (200 U) using random hexamers. Reverse transcribed products were amplified by RT-qPCR MasterMix (Life Technologies) and TaqMan assays (Applied Biosystems, Hammon, NJ, USA) for each of the human genes tested. Actin was used as a housekeeping gene. Relative gene expression was calculated as $2^{-\Delta Ct}$ ($\Delta Ct = Ct$ of the target gene minus Ct of actin).

Western blot analysis

Confluent, serum-starved cells were treated with the appropriate conditions, quickly placed on ice, and washed with ice-cold phosphate-buffered saline. SDS-PAGE, transfer, and Western blotting were performed as described elsewhere [19].

Measurement of Procollagen type I secretion

Serum-deprived cells were treated with myostatin in the presence or absence of the JNK inhibitor, SP600125 for 48 h. At the end of the incubation, conditioned media were collected and stored at -20°C until assayed. Type I procollagen was measured using a C-peptide enzyme immunoassay kit (Takara Bio Inc., Otsu, Shiga, Japan).

RNA interference

Transfection of primary HSC was performed by Amaxa nucleofection technology (Amaxa, Koln, Germany) as previously described [20], using 100 nM small interfering RNA (siRNA) targeting JNK or TGF- β , or control non-targeting siRNA (all provided by Dharmacon Inc., Lafayette, CO). The efficiency of silencing was evaluated by immunoblotting (JNK) or RT-PCR (TGF- β).

In vivo studies

C57Bl/6 mice, 8 weeks of age, were purchased from Charles River Laboratories (Calco, Italy). All animals received humane care and experimental protocols were conducted according to International guidelines (Guide for the Care and Use of Laboratory Animals, NIH publication No. 86-23), after authorization by the local regulatory authorities. Two different models were employed. A first group of mice was administered a single intragastric dose (1 ml/kg) of CCl₄ diluted in mineral oil (1:5, v/v) and sacrificed after 24, 48, or 72 h. Control mice received an equal volume of mineral oil. In a second model, mice were fed either a high-fat diet deficient in methionine and

choline (MCD), or a control diet supplemented with methionine and choline (CD) for 10 weeks. Diets were from Laboratori Dottori Piccioni (Milan, Italy). At the end of the experimental procedures, mice were euthanized by exsanguination under anesthesia, livers were rapidly dissected out, snap frozen in liquid nitrogen and stored at -80°C for RNA extraction. At least five mice for each experimental condition were analyzed.

Immunohistochemistry

The source of human liver tissue was previously reported [21]. In addition, two animal models of chronic injury were analyzed. Mice were fed a MCD diet, as described above, or treated with chronic CCl_4 administration. This latter set of animals was administered 0.5 ml/kg CCl_4 two times a week for six weeks, and then sacrificed as indicated above. Staining was performed essentially as described elsewhere [22]. Antigen retrieval was performed by heating in citrate buffer, pH 6.0 at 98°C for 30 min. Non-specific signal was eliminated by peroxidase block for 10 min at room temperature. Primary antibody was incubated at room temperature (1 hour) at a 1:1000 dilution in a humidified chamber, followed by incubation with a Horseradish peroxidase (HRP)-conjugated secondary antibody for 20 min at room temperature. Antibody binding was revealed by 3,3'-diaminobenzidine and reaction was stopped by immersion of tissue sections in distilled water once the brown colour appeared. Tissue sections were counterstained by hematoxylin and mounted. All reagents for immunohistochemistry were from Dako.

Measurement of myostatin levels

Determination of the levels of myostatin in serum and in cytosolic fractions obtained from liver tissues was carried out in a mouse model of acute liver damage induced by CCl_4 administration, as described above. A mouse MSTN/GDF8/myostatin Elisa kit (LSBio, Seattle, WA, USA) was employed.

Statistical analysis

Data in bar graphs represent means \pm SD from at least three independent experiments. Luminograms are representative of at least three experiments with similar results. Statistical analysis was performed using Student's t test. P values <0.05 were considered significant).

Results

We first analyzed the expression of ActR2B, which binds myo-statin, in experimental models of liver injury and fibrosis. A single administration of carbon tetrachloride in mice induces an acute damage associated with activation of a transient repair process similar to the one activated during chronic liver injury [23]. At all timepoints tested after CCl₄ administration, gene expression of ActR2B was markedly and significantly increased compared to mice treated with vehicle (Fig. 1A). We next evaluated expression of ActR2B in a model of fibrosis associated with steatohepatitis, after administration of a diet deficient in methionine and choline for 10 weeks [24]. This model causes pericentral fibrosis similar to the one observed in nonalcoholic steatohepatitis. Expression of ActR2B was dramatically increased in mice administered the fibrogenic diet compared to those receiving the control diet, supplemented with methionine and choline (Fig. 1B). We also tested the expression of ActR2B at the tissue level using immunohistochemistry, in two mouse models of chronic liver injury (Fig. 1C). In mice chronically intoxicated with CCl₄, increased expression of ActR2B was evident in areas of inflammation and formation of the fibrotic septum. In mice fed a methionine and choline-deficient diet for 10 weeks, a diffuse increase in ActR2B expression was evident, also involving areas of pericentral fibrosis. To examine whether HSC, the major cellular players in the fibrogenic process, contribute to expression of ActR2B, we evaluated gene expression of this receptor in different preparations of primary human HSC and in LX-2, a human immortalized HSC line. HSC expressed detectable transcripts for ActR2B (Fig. 1D), which, however, were not regulated by exposure to recombinant myostatin for as long as 24 h (data not shown). To investigate the pattern of ActR2B expression in human liver tissue, samples from patients with NASH-related fibrosis were stained with specific antibodies (Fig. 1E). Specific staining was diffusely present in hepatocytes and within the fibrotic septum. Staining of serial sections with anti- α -smooth muscle actin antibodies, which detect activated HSC, demonstrated partial co-localization of the immunohistochemical signal, indicating that fibrogenic HSC contribute to ActR2B expression in the fibrotic liver (Fig. 1E). Collectively, these data indicate that the receptor for myostatin is upregulated in conditions associated with fibrogenic repair of liver tissue, and that HSC contribute to expression of ActR2B.

We then explored whether myostatin levels are modulated in conditions of experimental liver injury. In mice with acute liver injury caused by CCl₄ administration (Fig. 2A), serum levels of myostatin were significantly increased at early time points after toxin administration. In contrast, no significant differences were observed when myostatin levels were assayed in liver tissue lysates (Fig.

2B). Having shown that HSC express ActR2B, we next investigated whether myostatin modifies the biology of these cells after binding to its cognate receptor. Proliferation and migration of HSC are pivotal actions which contribute to their pro-fibrogenic phenotype, although cytokines may differentially regulate these processes. Exposure of LX-2 to myostatin resulted in a significant reduction in cell proliferation, as established measuring the cellular metabolic activity (Fig. 3A). In contrast, PDGF-BB, used as a positive control, significantly increased proliferation. Migration of HSC is critical to determine accumulation of fibrogenic cells in discrete areas of the hepatic acinus, resulting in deposition of scar tissue in different regions, according to the etiology of chronic liver disease. Exposure to increasing concentrations of myostatin resulted in a significant increase in cell migration, which was similar, at the 50 ng/ml concentration, to the one achieved in response to PDGF-BB, the most potent mitogenic stimulus for this cell type (Fig. 3B–C). Of note, comparable results were observed in LX-2, an immortalized human HSC line, and in primary HSC, albeit minor differences in the response to myostatin were observed.

Increased expression of factors implicated in matrix turnover is another characteristic of activated HSC, and is modulated by different soluble factors. We first tested whether myostatin has the ability to regulate the expression of type 1 procollagen, a fibrillar component of extracellular matrix abundant in the fibrotic liver. Exposure to myostatin resulted in a significant increase in procollagen expression (Fig. 4A). Of note, myostatin was also able to induce a significant increase in the secretion of procollagen 1 in the culture supernatant (Fig. 6). The expression of TGF- β 1, one of the most potent fibrogenic cytokine, was also significantly upregulated when HSC were exposed to myostatin (Fig. 4A). Finally, myostatin upregulated TIMP-1 gene expression, indicating that reduced matrix turnover could contribute to the fibrogenic effects of this factor (Fig. 4C). Taken together, these data indicate a direct profibrogenic role of myostatin, via induction of factors implicated in matrix turnover. ActR2B belongs to the TGF- β receptors superfamily, and the effects of myostatin are similar to those exerted by TGF- β on HSC. Moreover, myostatin increases expression of TGF- β 1 (Fig. 4B). To establish whether myostatin acts inducing an upregulation of TGF- β secretion by HSC, we silenced TGF- β -1 with siRNA and incubated the cells in the presence or absence of myostatin (Table 1). The effects of myostatin on both migration and proliferation of HSC were maintained after TGF- β -1 knockdown, indicating that increased expression of TGF- β 1 is not necessary for the mitogenic and anti-proliferative actions of myostatin. Modification of the biologic properties of HSC is dependent on specific changes in different intracellular signaling pathways [25]. We tested whether myostatin modifies the activation of kinases.

Fig. 3. Myostatin induces growth-inhibition and promotes migration in HSC. (A) Serum-deprived LX-2 were left untreated (white bars), exposed to different concentrations of myostatin (50 ng/ml, grey bars, 100 ng/ml,

black bars) or 10 ng/ml PDGF-BB (crossed-hatched bars, positive control) for 24, 48, and 72 h. Cell proliferation was determined by MTT assay. Results are expressed as optical density values. Data are mean \pm SD of three independent experiments. * $P < 0.05$ vs Cnt. (B–C) Migration of LX-2 (B) or primary HSC (C) in response to indicated concentration of myostatin was evaluated using Boyden chambers. Data are the mean \pm SD of four experiments. * $P < 0.05$ vs Cnt. implicated in the regulation of the fibrogenic phenotype of HSC. Exposure to myostatin resulted in a rapid and significant increase in the activation of JNK (Fig. 5A). In contrast, activation of ERK1/2, another member of the mitogen-activated protein kinase family, and of Akt (Fig. 5B), was only modestly upregulated by myostatin. We next analyzed the possible effects of myostatin on the activation of Smad3, an intracellular protein critically implicated in the regulation of extracellular matrix turnover. Phosphorylation of Smad3 on activation-specific residues was dramatically increased in cells incubated with myostatin (Fig. 5C). These results provide a link between myostatin and activation of intracellular pathways linked to expression of collagen and other matrix components. Activation of JNK represents a pathway associated with a pro-fibrogenic phenotype of HSC [26]. Thus, we focused on the role of this kinase in the processes triggered by myostatin in HSC. In the presence of SP600125, a specific inhibitor of JNK activation, the ability of myostatin to induce migration of HSC was markedly and significantly blunted (Fig. 6A–B). Noteworthy, comparable data were obtained in the LX-2 cell line and in primary human HSC. Moreover, SP600125 reduced secretion of procollagen type 1 in the culture medium of myostatin-stimulated HSC (Fig. 6C–D). To further support these findings, we performed genetic silencing of JNK using specific siRNAs. This strategy determined a 50% decrease in JNK abundance (Fig. 7A). In these conditions, exposure to myostatin was significantly less effective in causing migration of HSC (Fig. 7B). Taken together, these data provide evidence that JNK activation is necessary to mediate the effects of myostatin on the fibrogenic phenotype of HSC.

Discussion

This study provides the first demonstration of a direct link between myostatin, a myokine, and the process of hepatic fibrogenesis. We found that myostatin modulates several biologic actions of HSC relevant for the fibrogenic process, and specifically cell migration and expression of molecules implicated in matrix turnover, at the gene expression and protein levels. Of note, the effects of myostatin resembled those of TGF- β , a protein of the same superfamily. Similar to TGF- β , myostatin caused growth arrest of HSC, while it up-regulated several factors implicated in fibrogenesis [27]. Finally, increased procollagen secretion was detected in cells exposed

myostatin. While these actions resemble those elicited by TGF- β , myostatin appears to act in an independent fashion, as genetic knockdown of TGF- β 1 in HSC did not result in any changes in the effects of myostatin on cell migration or proliferation. Of note, data obtained in LX-2, an immortalized HSC line, were replicated in primary HSC, albeit with minor quantitative differences, providing additional evidence to the present results. Data obtained in the past decade has highlighted the important concept that the fibrogenic process may be modulated by stimuli generated outside the liver [28]. Adipokines, i.e. cytokines mainly expressed in the adipose tissue, include leptin and adiponectin, which regulate fibrogenesis and HSC biology in opposite fashions [29]. More recently, the possibility that alterations in the microbiota result in modulation of fibrosis has been experimentally proven [30]. Data provided herein provide the first, proof-of-concept evidence that myokines represent an additional family of factors potentially modulating fibrogenesis from outside the liver.

Several recent studies have highlighted the possibility that the muscle-liver axis is very likely to play a relevant role in the pathogenesis of the metabolic syndrome. Sarcopenia in patients with NAFLD correlates with the degree of liver damage, and specifically with fibrosis [31]. In addition, reduced muscle mass is a hallmark of patients with alcoholic liver disease, and is common in cirrhosis [32]. In these conditions, where myostatin has been shown to be elevated in the systemic circulation, this factor could be a relevant mediator of accelerated fibrogenesis. Circulating myostatin levels in healthy subjects are around 40 ng/ml [33], and therefore the concentrations used in our in vitro experiments (50–100 ng/ml) are in a similar range. Remarkably, very similar levels were found in the serum of control mice, whereas myostatin concentrations almost doubled in conditions of acute liver injury. Data obtained in this study also provide insight on the intra-cellular signaling pathways implicated in the transmission of the fibrogenic signal by myostatin in HSC. Primary HSC and LX-2 were found to express ActR2B, the specific receptor for myostatin, identifying HSC as a target of myostatin's action. HSC appeared to contribute to ActR2B expression also in human liver tissue from patients with NASH and fibrosis, although other cells were also positively stained for this receptor. We next focused on proteins of the MAPK family and on Akt, which have been shown to play relevant roles in mediating the effects of different fibrogenic factors [25]. Myostatin only modestly activated Akt, or members of the MAPK family such as ERK1/2 and p38 MAPK. In contrast, a marked and consistent activation of JNK was observed. JNK, and particularly JNK-1, has been shown to be implicated in the fibrogenic process, both in vitro and in animal models [26]. In particular, several studies have indicated the ability of JNK activation in HSC to activate downstream pathways, regulating multiple actions relevant for fibrogenesis, such as cell proliferation, oxidative stress, and expression of profibrogenic factors [34,35]. We used both a

pharmacologic approach with the specific inhibitor SP600125 and a genetic approach with JNK-1 knockdown by siRNA. In both cases, the ability of myostatin to induce cell migration and to upregulate collagen secretion was significantly reduced, both in LX-2 and in primary HSC. Remarkably, only limited evidence had previously linked myostatin with activation of JNK. In C2C12 murine myoblasts, exposure to myostatin activates JNK, which mediated the growth inhibitory signal induced by this cytokine [36]. As myostatin has been linked to fibrosis in other tissues, but not in the liver, data reported herein are the first example of a myostatin-JNK-myofibroblast axis regulating fibrogenesis. In other systems, myostatin has been linked to the biology of fibrogenic cells. Overexpression of myostatin in cardiomyocytes resulted in altered cardiac function in older mice and in interstitial fibrosis, through activation of the p38MAPK pathway [37]. Moreover, myostatin has been implicated in the pathogenesis of fibrosis in skeletal muscle, where it induces fibroblast proliferation and secretion of extracellular matrix [38] and increases fibroblast resistance to apoptosis [39], via activation of Smad and p38MAPK signaling. Myostatin also promoted the differentiation of muscle fibroblasts into myofibroblasts, and induced expression of TGF- β in myofibers [40]. In vivo, induction of muscular damage in myostatin-deficient mice was associated with increased regeneration and reduced fibrosis. Nonetheless, the fibrogenic action of myostatin does not appear to be limited to muscle tissue, as myostatin has been involved in the pathogenesis of experimental Peyronie's disease in the rat [41]. Myostatin was also found to be expressed in the skin, and myostatin-deficient mice showed reduced healing of cutaneous wounds due to impaired myofibroblast differentiation, resulting in delayed contraction of the wound [42]. The identification of myostatin as a mediator of fibrosis in other tissues supports our finding of its profibrogenic activity in hepatic myofibroblasts. A few limitations of this study must be acknowledged. In particular, the relevance of the myostatin system in vivo was only explored analyzing the expression of ActR2B in models of liver repair and fibrogenesis. While the marked upregulation of the myostatin receptor in conditions of fibrogenic liver injury argues in favor of a pathogenic role of this factor, it does not provide in vivo mechanistic evidence. On the other hand, this is not easy to obtain due to the limited availability of pharmacologic blockers of myostatin's action and to the fact that myostatin-deficient mice have a complex phenotype that makes it difficult to single out a direct profibrogenic effect. Nonetheless, extension of these studies with experiments modulating the actions of myostatin in vivo is warranted in the near future. In conclusion, we have shown that myostatin, a protein which inhibits growth of skeletal muscle, modulates the biologic properties of human HSC in a profibrogenic fashion, via activation of JNK. These data identify a novel muscle-to-liver pathway potentially implicated in the pathogenesis of hepatic fibrosis in conditions such as NAFLD and alcoholic liver disease.

References

- [1] Sharma M, McFarlane C, Kambadur R, Kukreti H, Bonala S, Srinivasan S. Myo-statin: expanding horizons. *IUBMB Life* 2015;67:589–600.
- [2] McPherron AC, Lawler AM, Lee SJ. Regulation of skeletal muscle mass in mice by a new TGF- β superfamily member. *Nature* 1997;387:83–90.
- [3] Fearon KC, Glass DJ, Guttridge DC. Cancer cachexia: mediators, signaling, and metabolic pathways. *Cell Metab* 2012;16:153–66.
- [4] Huang Z, Chen X, Chen D. Myostatin: a novel insight into its role in metabolism, signal pathways, and expression regulation. *Cell Signal* 2011;23:1441–6.
- [5] Wilkes JJ, Lloyd DJ, Gekakis N. Loss-of-function mutation in myostatin reduces tumor necrosis factor α production and protects liver against obesity-induced insulin resistance. *Diabetes* 2009;58:1133–43.
- [6] McPherron AC, Lee SJ. Suppression of body fat accumulation in myostatin-deficient mice. *J Clin Invest* 2002;109:595–601.
- [7] Milan G, Dalla Nora E, Pilon C, Pagano C, Granzotto M, Manco M, et al. Changes in muscle myostatin expression in obese subjects after weight loss. *J Clin Endocrinol Metab* 2004;89:2724–7.
- [8] Palsgaard J, Brons C, Friedrichsen M, Dominguez H, Jensen M, Storgaard H, et al. Gene expression in skeletal muscle biopsies from people with type 2 diabetes and relatives: differential regulation of insulin signaling pathways. *PLoS One* 2009;4:e6575.
- [9] Jornayvaz FR, Samuel VT, Shulman GI. The role of muscle insulin resistance in the pathogenesis of atherogenic dyslipidemia and nonalcoholic fatty liver disease associated with the metabolic syndrome. *Annu Rev Nutr* 2010;30:273–90.
- [10] Rosselli M, Lotersztajn S, Vizzutti F, Arena U, Pinzani M, Marra F. The metabolic syndrome and chronic liver disease. *Curr Pharm Des* 2014;20:5010–24.
- [11] Ahmed A, Wong RJ, Harrison SA. Nonalcoholic fatty liver disease review: diagnosis, treatment, and outcomes. *Clin Gastroenterol Hepatol* 2015;13:2062–70.
- [12] Ekstedt M, Hagstrom H, Nasr P, Fredrikson M, Stal P, Kechagias S, et al. Fibrosis stage is the strongest predictor for disease-specific mortality in NAFLD after up to 33 years of follow-up. *Hepatology* 2015;61:1547–54.
- [13] Angulo P, Kleiner DE, Dam-Larsen S, Adams LA, Bjornsson ES, Charatcharoen-witthaya P, et al. Liver fibrosis, but no other histologic features, is associated with long-term outcomes of patients with nonalcoholic fatty liver disease. *Gastroenterology* 2015;149, 389–397 e10.

- [14] Trautwein C, Friedman SL, Schuppan D, Pinzani M. Hepatic fibrosis: concept to treatment. *J Hepatol* 2015;62:S15–24.
- [15] Mederacke I, Hsu CC, Troeger JS, Huebener P, Mu X, Dapito DH, et al. Fat tracing reveals hepatic stellate cells as dominant contributors to liver fibrosis independent of its aetiology. *Nat Commun* 2013;4:2823.
- [16] Wallace MC, Friedman SL, Mann DA. Emerging and disease-specific mechanisms of hepatic stellate cell activation. *Semin Liver Dis* 2015;35:107–18.
- [17] Petta S, Valenti L, Marra F, Grimaudo S, Tripodo C, Bugianesi E, et al. MERTK rs4374383 polymorphism affects the severity of fibrosis in non-alcoholic fatty liver disease. *J Hepatol* 2016;64:682–90.
- [18] Di Maira G, Brustolon F, Tosoni K, Belli S, Kramer SD, Pinna LA, et al. Comparative analysis of CK2 expression and function in tumor cell lines displaying sensitivity vs. resistance to chemical induced apoptosis. *Mol Cell Biochem* 2008;316:155–61.
- [19] Rovida E, Di Maira G, Tusa I, Cannito S, Paternostro C, Navari N, et al. The mitogen-activated protein kinase ERK5 regulates the development and growth of hepatocellular carcinoma. *Gut* 2015;64:1454–65.
- [20] Caligiuri A, Bertolani C, Guerra CT, Aleffi S, Galastri S, Trappoliere M, et al. Adenosine monophosphate-activated protein kinase modulates the activated phenotype of hepatic stellate cells. *Hepatology* 2008;47:668–76.
- [21] Locatelli I, Sutti S, Jindal A, Vacchiano M, Bozzola C, Reutelingsperger C, et al. Endogenous annexin A1 is a novel protective determinant in nonalcoholic steatohepatitis in mice. *Hepatology* 2014;60:531–44.
- [22] Carloni V, Lulli M, Madietti S, Mello T, Hall A, Luong TV, et al. CHK2 overexpression and mislocalisation within mitotic structures enhances chromosomal instability and hepatocellular carcinoma progression. *Gut* 2018;67:348–61.
- [23] Marra F, Gentilini A, Pinzani M, Choudhury GG, Parola M, Herbst H, et al. Phosphatidylinositol 3-kinase is required for platelet-derived growth factor's actions on hepatic stellate cells. *Gastroenterology* 1997;112:1297–306.
- [24] Vizzutti F, Provenzano A, Galastri S, Milani S, Delogu W, Novo E, et al. Curcumin limits the fibrogenic evolution of experimental steatohepatitis. *Lab Invest* 2010;90:104–15.
- [25] Caligiuri A, Marra F. Stellate cells. In: Dufour JF, Clavien PA, editors. *Signaling pathways in liver diseases*. Chichester: John Wiley & Sons; 2015. p. 34–60.
- [26] Seki E, Brenner DA, Karin M. A liver full of JNK: signaling in regulation of cell function and disease pathogenesis, and clinical approaches. *Gastroenterology* 2012;143:307–20.

- [27] Friedman SL. Hepatic stellate cells: protean, multifunctional, and enigmatic cells of the liver. *Physiol Rev* 2008;88:125–72.
- [28] Caligiuri A, Gentilini A, Marra F. Molecular pathogenesis of NASH. *Int J Mol Sci* 2016;17.
- [29] Marra F, Bertolani C. Adipokines in liver diseases. *Hepatology* 2009;50:957–69.
- [30] De Minicis S, Rychlicki C, Agostinelli L, Saccomanno S, Candelaresi C, Trozzi L, et al. Dysbiosis contributes to fibrogenesis in the course of chronic liver injury in mice. *Hepatology* 2014;59:1738–49.
- [31] Petta S, Ciminnisi S, Di Marco V, Cabibi D, Camma C, Licata A, et al. Sarcopenia is associated with severe liver fibrosis in patients with non-alcoholic fatty liver disease. *Aliment Pharmacol Ther* 2017;45:510–8.
- [32] Dasarathy S, Merli M. Sarcopenia from mechanism to diagnosis and treatment in liver disease. *J Hepatol* 2016;65:1232–44.
- [33] Gruson D, Ahn SA, Ketelslegers JM, Rousseau MF. Increased plasma myostatin in heart failure. *Eur J Heart Fail* 2011;13:734–6.
- [34] Novo E, Povero D, Busletta C, Paternostro C, di Bonzo LV, Cannito S, et al. The biphasic nature of hypoxia-induced directional migration of activated human hepatic stellate cells. *J Pathol* 2012;226:588–97.
- [35] Fabre T, Kared H, Friedman SL, Shoukry NH. IL-17A enhances the expression of profibrotic genes through upregulation of the TGF- β receptor on hepatic stellate cells in a JNK-dependent manner. *J Immunol* 2014;193:3925–33.
- [36] Huang Z, Chen D, Zhang K, Yu B, Chen X, Meng J. Regulation of myostatin signaling by c-Jun N-terminal kinase in C2C12 cells. *Cell Signal* 2007;19:2286–95.
- [37] Biesemann N, Mendler L, Kostin S, Wietelmann A, Borchardt T, Braun T. Myostatin induces interstitial fibrosis in the heart via TAK1 and p38. *Cell Tissue Res* 2015;361:779–87.
- [38] Li ZB, Kollias HD, Wagner KR. Myostatin directly regulates skeletal muscle fibrosis. *J Biol Chem* 2008;283:19371–8.
- [39] Bo Li Z, Zhang J, Wagner KR. Inhibition of myostatin reverses muscle fibrosis through apoptosis. *J Cell Sci* 2012;125:3957–65.
- [40] Zhu J, Li Y, Shen W, Qiao C, Ambrosio F, Lavasani M, et al. Relationships between transforming growth factor- β 1, myostatin, and decorin: implications for skeletal muscle fibrosis. *J Biol Chem* 2007;282:25852–63.
- [41] Cantini LP, Ferrini MG, Vernet D, Magee TR, Qian A, Gelfand RA, et al. Profibrotic role of myostatin in Peyronie's disease. *J Sex Med* 2008;5:1607–22.
- [42] Zhang C, Tan CK, McFarlane C, Sharma M, Tan NS, Kambadur R. Myostatin-null mice exhibit delayed skin wound healing through the blockade of transforming growth factor- β signaling by decorin. *Am J Physiol Cell Physiol* 2012;302:C1213–25.

Tables

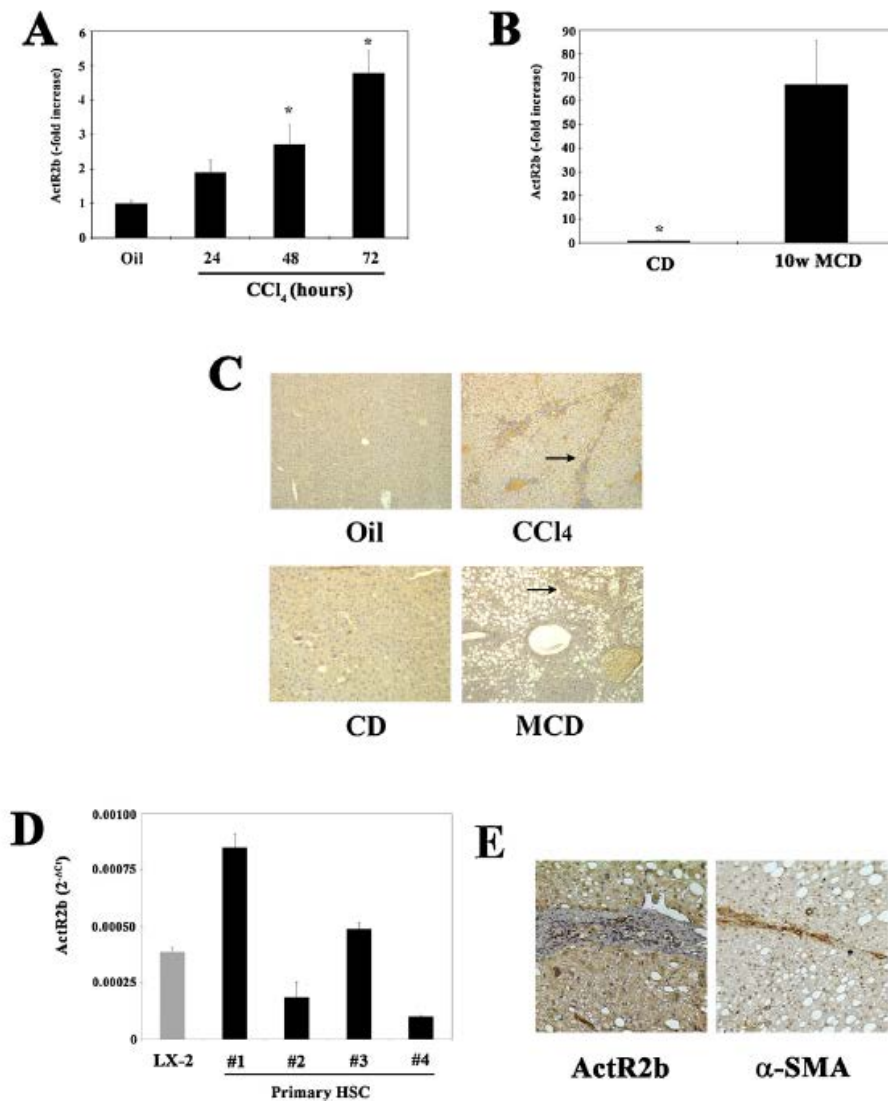
Table 1. Effects of TGF-B- B1 silencing on myostatin-induced proliferation and migration of HSC.

A					
	48 h	72 h			
TGF-β1 mRNA(-fold change over NT siRNA)	0.18 ± 0.18 [†]	0.07 ± 0.18 [†]			
B					
	Non-targeting siRNA		TGFβ1 siRNA		
	Control	Myostatin	Control	Myostatin	
Migration (cells/HPF)		8.8 ± 5.5 ^a	35.4 ± 12.5 ^b	5.3 ± 2.4 ^b	31.6 ± 19.2
Proliferation (MTT arbitrary units)		417 ± 138 ^a	406 ± 140 ^c	360 ± 90 ^d	325 ± 87

(A): LX-2 cells were transfected with siRNA for the indicated time points, and gene expression of cells transfected with siRNA directed against TGF-B1 was compared to the one of cells transfected with non-targeting siRNA. (B) LX-2 cells were transfected with siRNA as indicated, and incubated in the presence or absence of 50 ng/ml myostatin. Analysis of cell migration and proliferation were performed as described in Materials and Methods. aP < 0.05 vs. myostatin and non-targeting siRNA. bP = 0.07 vs. myostatin and TGF-B1 siRNA. cP = NS vs. myostatin and TGF-B1 siRNA. dP < 0.05 vs. myostatin and TGF- B1 siRNA. HPF, high-power field. *P < 0.01.

Figures

Fig. 1. Hepatic expression of the myostatin receptor ActR2B in experimental liver injury, in human HSC, and in human liver tissue.



(A) C57Bl/6 mice ($n \geq 3$) were orally administered CCl₄ (1 ml/kg) or vehicle (olive oil) for the indicated time periods. (B) C57Bl/6 mice ($n \geq 3$) were fed a methionine and choline deficient diet (MCD) or a control diet (CD) for 10 weeks. Total RNA was isolated from liver tissue and the expression of ActR2B was determined by qRT-PCR. Target gene expression was normalized to GAPDH. Data are expressed as -fold increase over control. * $P < 0.05$ vs. control. (C) Top panels: mice were treated with mineral oil or with CCl₄ for 6 weeks, as described in Materials and Methods. Bottom panels: mice were fed with a control diet (CD) or a diet deficient in methionine and choline (MCD) for 10 weeks. Slides were stained with antibodies against ActR2B. Arrows indicate areas of fibrogenesis. (D) Total RNA was isolated from the human HSC line, LX-2, and from different preparations of primary HSC. mRNA expression of ActR2B was evaluated by qRT-PCR. Relative gene expression was calculated as $2^{-\Delta C_t}$ ($\Delta C_t = C_t \text{ of the target} - C_t \text{ of } \beta\text{-actin}$). (E) Serial

sections of liver tissue from a patient with NASH and fibrosis were stained with antibodies against ActR2b (left) or α -smooth muscle actin (right), a marker of activated HSC. Brown color shows partial co-localization between the two stainings in the fibrotic septum.

Fig. 2. Serum and hepatic levels of myostatin in conditions of liver injury. Mice were treated with mineral oil (control) or with a single intragastric administration of 1.0 ml/kg CCl₄ and sacrificed after the indicated periods of time. Myostatin levels were analyzed in serum (A) and in tissue lysates (B) as indicated in Materials and Methods. Data are mean \pm SD of at least three mice per group. *P < 0.05 vs. control (Oil).

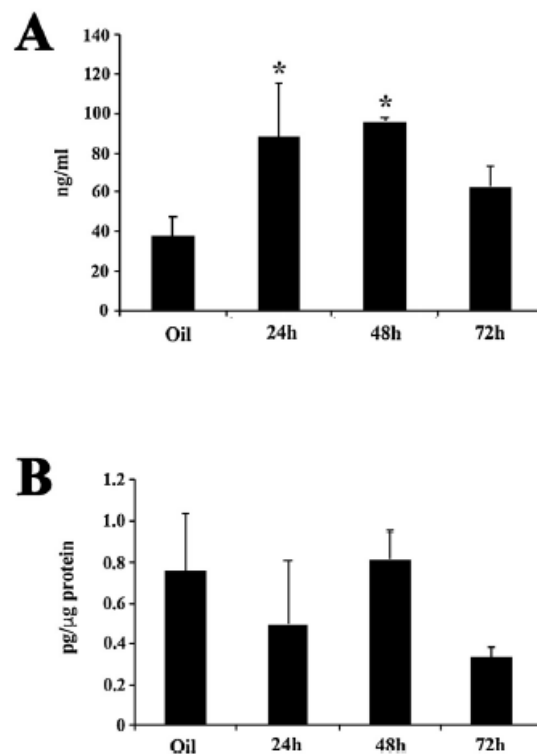
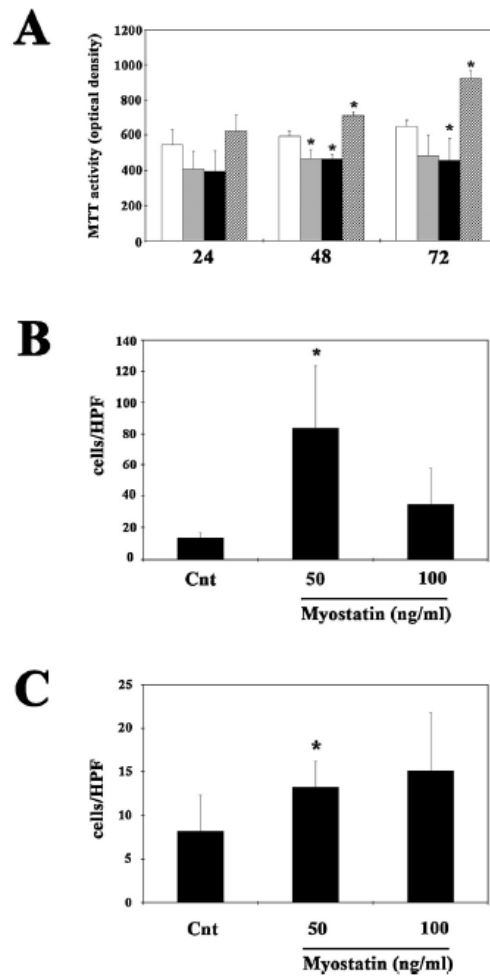
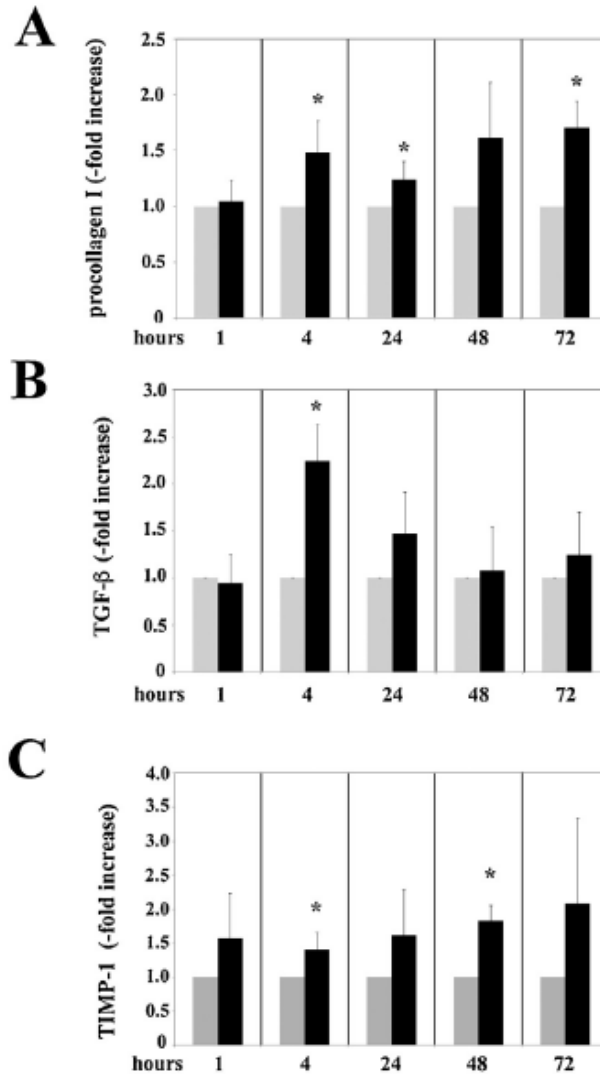


Fig. 3. Myostatin induces growth-inhibition and promotes migration in HSC.



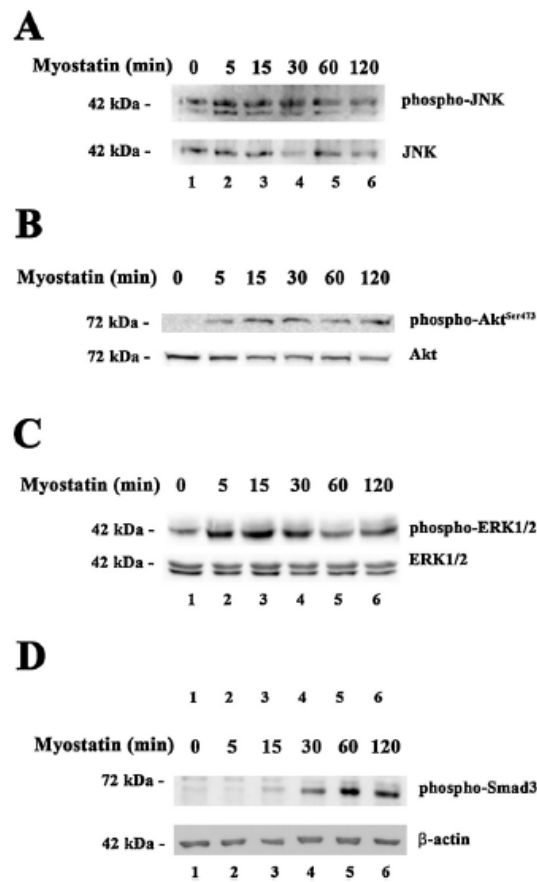
(A) Serum-deprived LX-2 were left untreated (white bars), exposed to different concentrations of myostatin (50 ng/ml, grey bars, 100 ng/ml, black bars) or 10 ng/ml PDGF-BB (crossed-hatched bars, positive control) for 24, 48, and 72 h. Cell proliferation was determined by MTT assay. Results are expressed as optical density values. Data are mean \pm SD of three independent experiments. * $P < 0.05$ vs Cnt. (B–C) Migration of LX-2 (B) or primary HSC (C) in response to indicated concentration of myostatin was evaluated using Boyden chambers. Data are the mean \pm SD of four experiments. * $P < 0.05$ vs Cnt.

Fig. 4. Myostatin positively modulates the expression of profibrogenic genes.



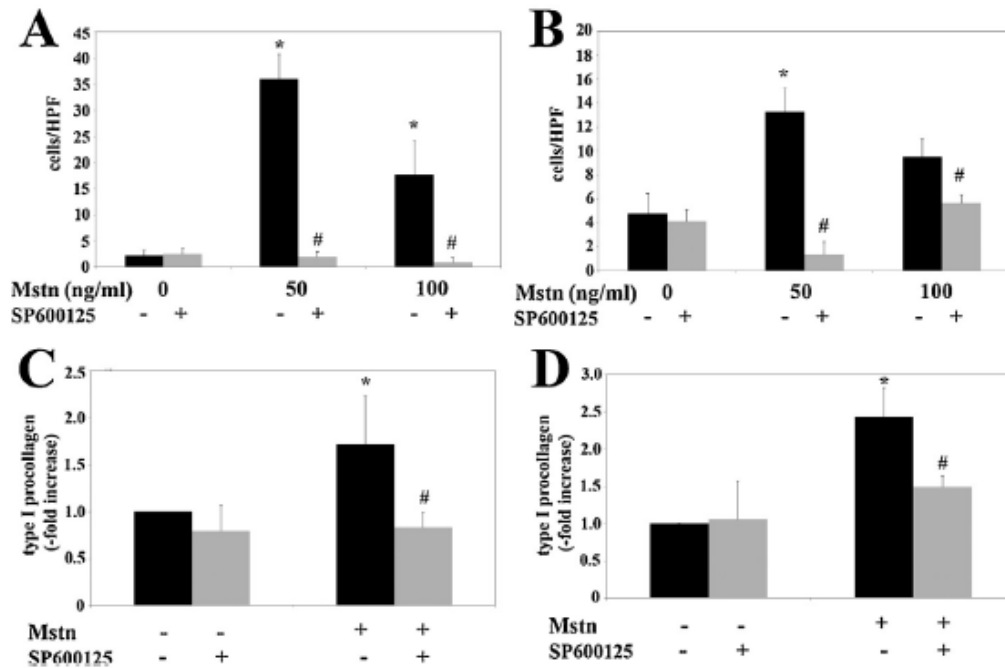
Serum-deprived LX-2 were incubated in the presence (black columns) or in the absence (gray columns) of 50 ng/ml myostatin for the indicated time points. Total RNA was extracted and the expression of procollagen 1 (A), TGF- β 1 (B) and TIMP-1 (C) was determined by qRT-PCR. Target gene expression was normalized to actin. Results, expressed as fold increase over control, represent the mean value \pm SD of three independent experiments. * $P < 0.05$ vs the same time point in the absence of myostatin.

Fig. 5. Signaling pathways activated by myostatin.



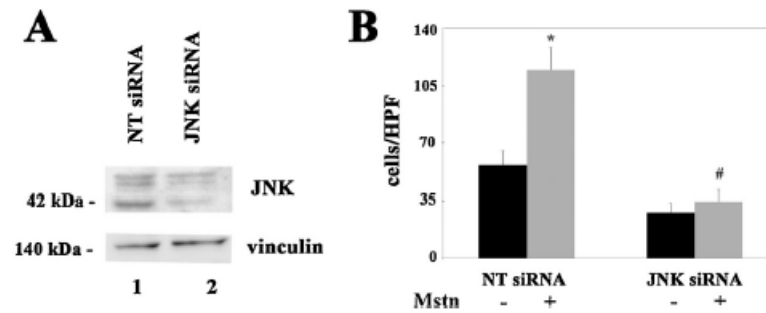
Serum-starved LX-2 cells were exposed to 50 ng/ml myostatin for the indicated time points. Total cell lysates were analyzed by immunoblotting using antibodies directed against the phosphorylated forms of JNK (A), Akt (B) ERK1/2 (C) or Smad-3 (D). Data from a single experiment representative of at least three with similar results.

Fig. 6. Biologic effects of myostatin in HSC are blocked by a JNK inhibitor.



(A–B) Migration of LX-2 cells (A) or primary HSC (B) in response to myostatin (50–100 ng/ml) was evaluated in the presence or absence of the JNK inhibitor SP600125 (20 μ M), using Boyden chambers. Data are the mean \pm SD of three independent experiments. (C–D) Serum-starved LX-2 cells (C) or primary HSC (D) were treated with myostatin (50 ng/ml) in the presence or absence of 20 μ M SP600125 for 48 h. Procollagen type I secretion was determined in cell supernatants by EIA. Results were normalized for total protein content in cell lysates. Data are expressed as fold change over control and indicate the mean \pm SD of three independent experiments. * P < 0.05 vs Cnt; # P < 0.05 vs myostatin (Mstn).

Fig. 7. JNK is required for myostatin-induced biological actions in HSC.



Knockdown of JNK in primary HSC was achieved by transfection of specific siRNA (JNK siRNA). Non-targeting siRNA (NT siRNA) were employed as control. (A) Transfection efficiency was evaluated by Western blotting using antibodies against JNK or vinculin, as control for equal loading. Data from a single experiment representative of three. (B) Cell migration in response to 50 ng/ml myostatin was tested in serum-starved HSC, 48 h following transfection. Data are the mean \pm SD of three independent experiments. * $P < 0.05$ vs Cnt; # $P < 0.05$ vs NT siRNA + myostatin (Mstn).